

# **Dynamic Atomic Force Microscopy Analysis of Polymer Materials: Beyond Imaging Their Surface Morphology**

**Ph. Leclère<sup>1,2</sup>, V. Cornet<sup>1</sup>, M. Surin<sup>1</sup>, P. Viville<sup>1</sup>,  
J. P. Aimé<sup>2</sup>, and R. Lazzaroni<sup>1</sup>**

**<sup>1</sup>Service de Chimie des Matériaux Nouveaux, Université de Mons-Hainaut.  
Materia Nova, Place du Parc 20, B-7000 Mons, Belgium**

**<sup>2</sup>CPMOH, Université de Bordeaux I, 351 Cours de la Libération, F-33405  
Talence Cedex, France**

Dynamic atomic force microscopy is known for its ability to image soft materials without inducing severe damage. The understanding of the origin of the image contrast is not obvious and constitutes an important subject of debate. Here, we propose a straightforward method, based on the analysis of approach-retract curves, which provides an unambiguous quantitative measurement of the local mechanical response and/or topographic contribution(s), depending on the studied sample. From the recorded data, we show that it is possible to determine the different contributions and, therefore, go beyond the morphological aspects. This approach is illustrated here on a thermoplastic elastomer block copolymer, used as a model system presenting phase-separated nanodomains characterized by specific mechanical properties. The extension of the technique to other polymer systems, such as polymer blends, polymer nanocomposites, and conjugated materials, is also discussed.

## Introduction

The development of nanotechnology implies a large effort to study and understand physical phenomena at the nanometer scale. Methods using local force probes provide important contributions to those studies, because the small size of the tip allows one to probe surfaces with excellent lateral and vertical resolution. Among those scanning microscopies, dynamical force techniques, *i.e.*, using an oscillating tip, are particularly well adapted to soft samples such as polymers or biological systems. Among many applications of those techniques, one convincing illustration of their potential is the advance brought to microstructural studies of block copolymers by phase imaging in Tapping mode Atomic Force Microscopy [1-7].

In dynamical modes, two types of operation are possible: either the oscillating amplitude is fixed and the output signal is the resonance frequency (this is called the non-contact resonant force mode [8]), or the oscillation frequency is fixed and the variations of the amplitude and phase are recorded. This mode is commonly named tapping-mode (also known as intermittent contact mode [9]) and is the one that is considered in this study. Tapping-mode (TMAFM) is commonly used because of its ability to probe soft samples, due to the minimization of sample damage during the scanning. Moreover, tapping-mode images can be of two different types: in one type, the image corresponds to the changes of the piezoactuator height necessary to maintain a fixed oscillation amplitude through a feedback loop (the height image); in the other type, the image contains the changes of the oscillator phase delay relative to the excitation signal (phase image). This additional imaging possibility has revealed in many cases a high sensitivity to variations of the local properties. A number of studies have shown the possibility to extract useful information from tapping-mode images of soft samples, especially with samples showing a particular contrast on the local scale, like blends of hard and soft materials [5, 10].

Nevertheless, important questions remain about the physical origin of the image contrast in tapping mode [11-13]. In many cases, the height images are considered to display topographic information, but it must be kept in mind that the local mechanical properties of the samples (*i.e.*, the possibility that the tip slightly penetrates the surface) may also contribute to contrast in the height image. For the phase image, in the dominant repulsive regime, the phase shifts are related to the local mechanical properties. At this point, it is worth mentioning that, in order to maintain the tip in a well-defined oscillating behavior, the perturbation to the oscillator due to the contact with the surface is chosen to be small; in other words, the reduction of the free amplitude (the set-point) is only of a few percent. This method has two advantages: from an experimental point of view, this allows one to identify immediately hard and soft domains, the bright parts of the image

corresponding to hard domains. From a theoretical point of view, this allows us to use simple approximations providing analytical solutions able to fit the experimental data [5, 13].

Here, we propose a straightforward method, based on the analysis of approach-retract curves, to provide an unambiguous quantitative measurement of the local mechanical response and/or topographic contribution(s), depending on the studied sample. Moreover, a step further in the understanding of the image contrast is proposed, *via* the analysis of the variation of the phase as a function of the tip-surface distance. The fitting of the experimental data by an appropriate model provides a quantitative evaluation of the contribution of topography, adhesion, indentation and dissipation processes to the contrast. This approach is first applied to thin films of thermoplastic elastomer block copolymers, which are known to phase-separate into well-defined domains on the nanometer scale. The method is extended to other polymer systems, such as polymer blends and polymer nanocomposites.

## **Experimental Results**

### **Thermoplastic Elastomers as Model Systems**

A key point for soft materials is a proper interpretation of the observed contrast. In most cases one has to discriminate between the respective contributions of: (i) the actual topography and (ii) the difference in mechanical properties to the height images. Here, we review a straightforward and easy experimental method to evaluate the contribution of the local mechanical properties to the image contrast. Our approach is based on the reconstruction of height or phase image sections via a rapid analysis of approach-retract curves recorded along those section lines. As recently described [5], a comparison between recorded images and the set of approach-retract curves provides an easy way to discriminate between the topographic and mechanical contributions.

The model system is a thin film of a thermoplastic elastomer, *i.e.*, a block copolymer in which the chemical structure of the sequences is designed in such a way that (i) phase separation of the sequences occurs, giving a well-defined spatial distribution of domains at the nanometer scale and (ii) the domains containing different sequences possess different mechanical properties [5, 6]. Here, the chemical composition has been selected to produce a lamellar morphology. In this case, AFM pictures of a PMMA-*b*-poly(alkylacrylate)-*b*-PMMA film present an alternating array of rubbery and glassy lamellae, with a periodicity of 27 nm, as shown in Figure 1.

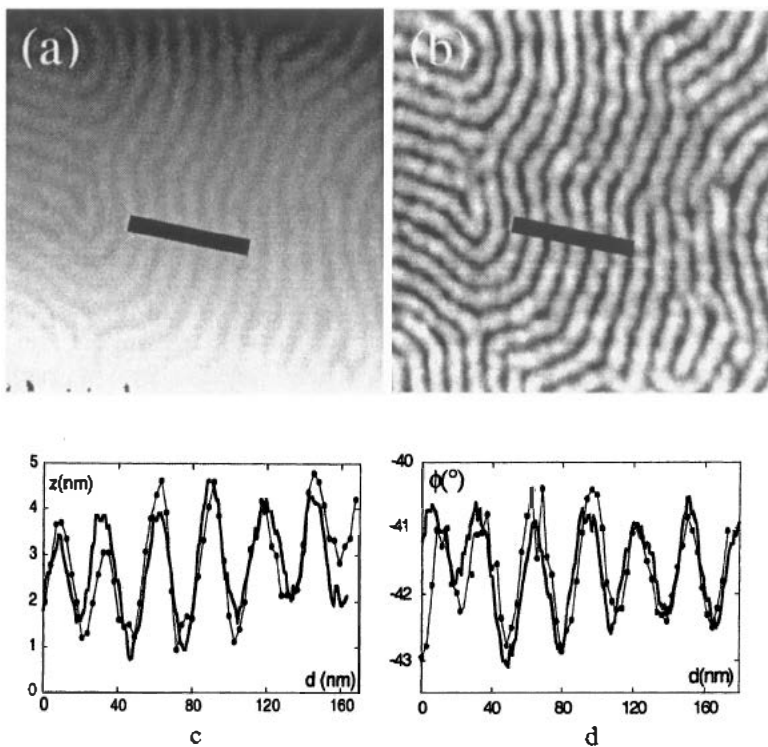


**Figure 1.** Tapping-mode AFM images ( $1.0 \times 1.0 \mu\text{m}^2$ ) of a PMMA-*b*-poly(alkylacrylate)-*b*-PMMA film: (a) Height image (b) Phase; Comparison of the image sections with the profiles built from the approach-retract curves data [13]: (c) Height image; (d) Phase image.

The correspondence between the two sets of data (same behavior for the topographic section, not shown here) appears to be very good. This agreement means that for those copolymers, the contrast in the height image is related to different oscillator responses on the glassy and elastomer domains, with no discernible topographic contribution to the contrast. Therefore, the contrast is mostly due to changes in the sample local mechanical properties.

From tapping-mode images of block copolymers, it is not only possible to describe the morphology corresponding to the nanophase separation occurring between the specific domains but also to evaluate accurately the respective contributions of the topography and the mechanical properties. In this case, we can also propose that the phase contrast can be explained on the basis of the viscous forces acting against the tip motion during the indentation of the tip in the sample [13-15].

### **Applications to other polymer materials.**

**Biodegradable Polymer Blends.** In this section, we extend the concept to polymer blends made of biodegradable and biocompatible components, namely PMMA and poly( $\epsilon$ -caprolactone)(PCL). These blends are in current development for biomedical applications such as drug release systems or prostheses [16]. Figure 2a illustrates the topographic image of a 75:25 weight % PMMA/PCL blend as a thin film. From the section analysis (Figure 2b) and the bearing analysis (not shown here) of the topographic image, it appears that the dark areas, corresponding to the softer component (*i.e.*, the PCL domains), are located approximatively 60 nm below the bright (mechanically harder) zones.

Approach-retract curves recorded on different domains on the polymer blend sample surface are markedly different: the slope of the amplitude/distance curve is 0.75 for the harder, glassy domains while it is smaller (0.60) on the softer domains, meaning that, for the same set-point, there is larger tip indentation in the softer domains. Using the same procedure as described for the block copolymer, we measure a difference of about 15 nm between the lowest points in the image section and the corresponding reconstruction (Figure 2b). Therefore, from these data (160 points), it appears that, in this case, an indentation of about 15 nm in the PCL softer domain has to be considered to fit the experimental data. Note that, at room temperature, the PCL is largely above its glass temperature transition ( $T_g = -60^\circ\text{C}$ ). Therefore, the 60 nm height difference recorded in the height images actually corresponds to a 15 nm indentation into PCL domains that are actually 45 nm below the level of the PMMA domains. This height difference probably originates from the film formation process from the solution of the two polymers in a common solvent. The topographic modulation can be explained by a different rate of solvent evaporation during the film drying process for the two phases [17].

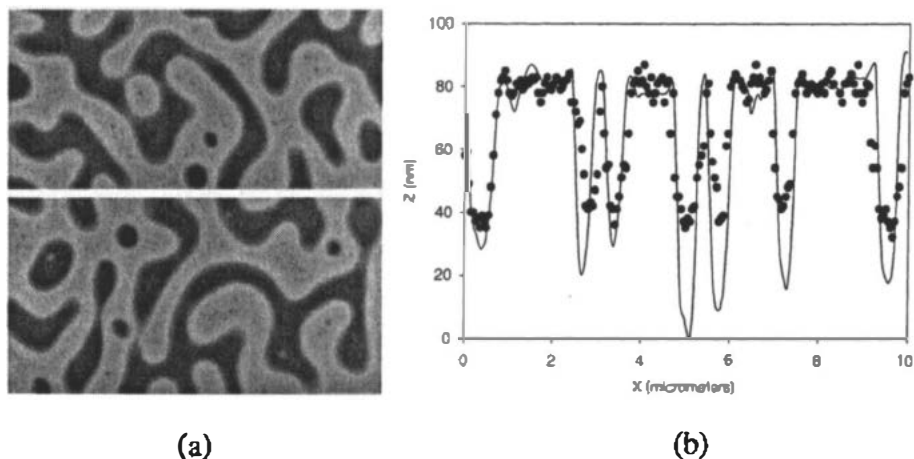


**Figure 2.** (a) Tapping-mode AFM height image ( $8.0 \times 8.0 \mu\text{m}^2$ ) of a PMMA-PCL co-continuous polymer blend (75:25) film. The vertical scale is 80 nm; (b) Image section and its reconstruction from approach-retract curve analysis. The solid line corresponds to the image section and the black dots are the reconstructed data.

**Conjugated polymers.** We also applied this technique to conjugated organic semiconducting materials. Compared to inorganic materials, conjugated polymers have the advantages of easy control of the semiconducting properties through chemical modification, and ease of processing over large areas, leading to major potential cost savings in device manufacture. LEDs and transistors based on conjugated materials are now being actively developed for commercial applications. Generally, when conjugated oligomers or polymers are deposited from a molecularly dissolved solution on a substrate, like muscovite mica, HOPG or silicon wafers, they tend to form fibrils by self-assembling processes governed by  $\pi$ -stacking of the polymer chains [18-20]. In the present case, the conjugated oligomer is made of about 20 units of indenofluorene (Figure 3). This polymer is a well-known efficient blue emitter for LEDs. Upon annealing at  $300^\circ\text{C}$  (above the liquid crystal transition temperature of  $270^\circ\text{C}$ ), the polymer reorganizes in such a way that the fibrillar morphology is no more present. Figure 4 illustrates the typical morphology observed by AFM after annealing. The analysis of the height image shows a difference of 18 nm between the upper (brighter) layer and the lower (darker) layer. From the phase image (vertical grey scale 1.0 degree) there is no significant contrast between the two layers (only the contours of the cavities are visible).

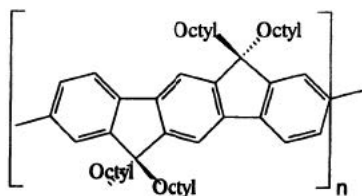
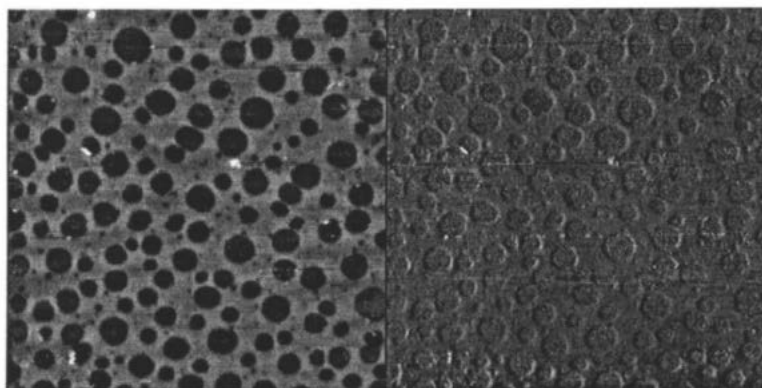
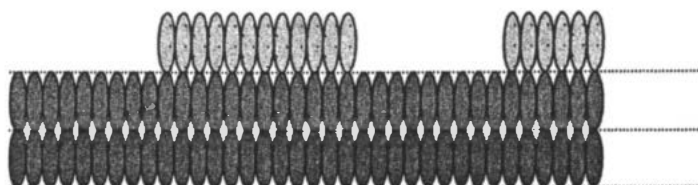


**Figure 3.** Chemical structure of oligo indenofluorene ( $n= 20-22$ ).



(a)

(b)



(c)

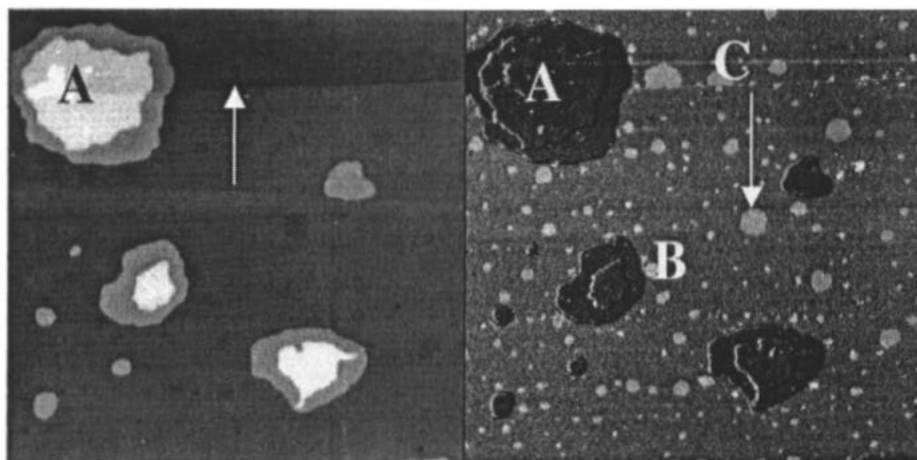
**Figure 4.** (a) Tapping-mode AFM height image ( $30.0 \times 30.0 \mu\text{m}^2$ ) of an oligo indenofluorene thin deposit. The vertical scale is 100 nm; (b) Corresponding phase image. The vertical scale is 1.0 degree; (c) Proposed model for the molecular organization within the film.

The length of the extended indenofluorene oligomer with 20 units is estimated to be around 18.5 nm. This strongly suggests that the layers are made of molecules standing up perpendicularly to the substrate, as depicted in Figure 4c. The fact that the phase contrast between the different layers is very low means that the tip is probing the same material or at least material with the same mechanical properties. For this sample, approach retract curves are strictly identical whatever the location on the sample. This implies that the contrast observed on the height image is purely topographic.

Figure 5 illustrates the morphology adopted by ar conjugated oligomer based on six thiophene units substituted on one end by a short poly(ethylene oxide) segment (Figure 5c). These molecules are deposited on a freshly cleaved HOPG substrate. On the height image, we clearly see a molecular step (indicated by the arrow on Figure 5a). The thickness of brighter islands (indicated by an "A" on Figure 5a) is about 6.0 nm, which roughly corresponds to length of the fully extended molecule. The islands are thus two-dimensional assemblies in which the molecules are perpendicular to the substrate (or slightly tilted). This interpretation is fully confirmed by the phase image, on which the islands show the same phase lag (*i.e.*, the same dark color). Small white spots are also visible (indicated by "C" on Figure 5b). STM analysis of the same sample indicates that this zone is actually the HOPG surface while the light gray zone ("B" on Figure 5b) is made of a monolayer of molecules lying flat. The phase of the oscillating tip is different enough when the tip is over the monolayer, or over an island, or over the HOPG, so that it is possible to understand the nature of the three distinct zones in the AFM image.

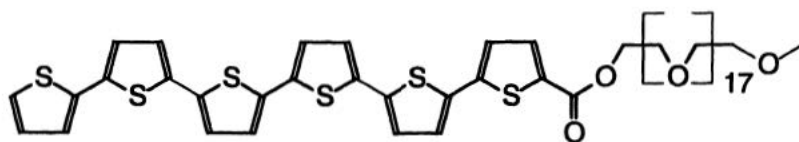
**Nanocomposites.** This work deals with the preparation and the surface characterization of biodegradable nanocomposites made of poly( $\epsilon$ -caprolactone) (PCL) and Montmorillonite-type clay. Nanocomposites with different relative compositions of PCL and Montmorillonite, either natural or organo-modified by various alkylammonium cations, are prepared by melt intercalation and in situ intercalative polymerization [22, 23]. The goal of this study is to characterize the dispersion of the clay layers in the PCL matrix, which is a critical parameter governing the final physical properties of the obtained nanocomposites. Figure 6a shows a TMAFM image of the sample, where flat elongated objects are dispersed in the matrix. On Figure 6b, we can clearly see that the approach curves on zone A and B are drastically different. On zone A, the slope is around 0.99 and is much larger than for zone B (slope = 0.52).





(a)

(b)



(c)

**Figure 5. (a) Tapping-mode AFM height image ( $30.0 \times 30.0 \mu\text{m}^2$ ) of T6-(EO)<sub>18</sub> thin deposit on HOPG from THF solution. The vertical scale is 25 nm; (b) Corresponding phase image. The vertical scale is 10 degree; (c) Chemical structure of the oligothiophene molecule.**

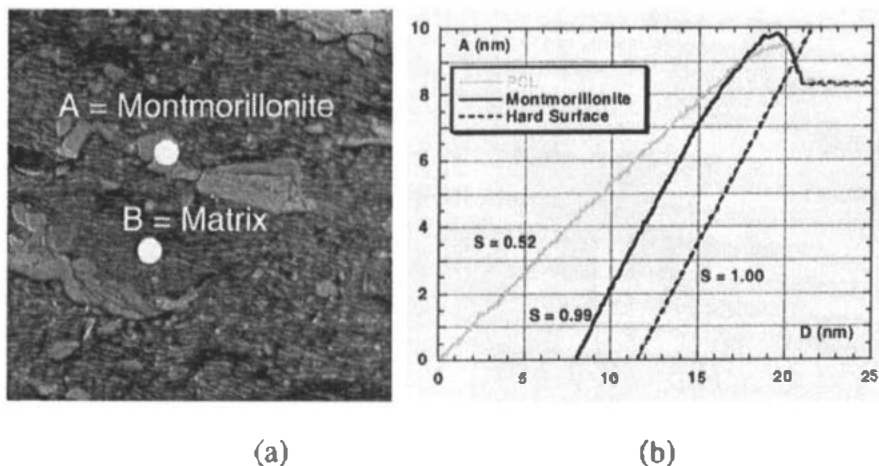


**Figure 6.** (a) Tapping-mode AFM phase image ( $1.0 \times 1.0 \mu\text{m}^2$ ) of a Montmorillonite-PCL nanocomposite; (b) Experimental approach-retract curves recorded over the PCL matrix and clay inclusions.

A slope value close to unity is the typical signature of a very hard surface (see model curve on Figure 6b), because it corresponds to a situation where no tip indentation takes place. In contrast, a slope value significantly lower than 1 indicates that the tip indents the surface (hence, its oscillation amplitude decreases more slowly than on a hard surface). Thus, we can easily assign the two components from their mechanical responses [18]: zone A is made of Montmorillonite layers while zone B is the PCL matrix. This example illustrates the usefulness of approach-retract curve analysis in the description of the surface morphology.

## Conclusions

Here we described a simple and straightforward method (based on the analysis of approach-retract curves) to: (i) give a quantitative estimation of the topographic and the mechanical contribution to height and phase images; (ii) assign the various

components in image of heterogeneous polymer materials. This technique has been successively used for pure topographic or pure mechanical contrast as well as for samples with a mixing of the two contributions to the height and phase AFM images.

## Acknowledgements

The authors are grateful to J. D. Tong and R. Jérôme (CERM, University of Liège, Belgium) for the synthesis of the triblock copolymers. Conjugated polymers were kindly provided by K. Müllen (MPI-P, Mainz, Germany) and W.J. Feast (IRC Durham, UK). Research in Mons is partially supported by the Belgian Science Policy Program "Pôle d'Attraction Interuniversitaire en Chimie Supramoléculaire et Catalyse Supramoléculaire" (PAI 5/3), the European Commission and the Government of the Région Wallonne (Phasing Out Program). Research in Bordeaux is supported by the Conseil Régional d'Aquitaine. M.S. acknowledges the F.R.I.A. (Belgium) for a doctoral scholarship.

## References

1. Leclère, Ph.; Lazzaroni, R.; Brédas, J.L.; Yu, J.M.; Dubois, Ph.; Jérôme, R. *Langmuir* **1996**, *12*, 4317.
2. Stocker, W.; Beckmann, J.; Stadler, R.; Rabe, J.P. *Macromolecules* **1996**, *29*, 7502.
3. Magonov, S.N.; Elings, V.; Wangbo, M.H. *Surf. Sci.* **1997**, *389*, 201.
4. Leclère, Ph.; Moineau, G.; Minet, M.; Dubois, Ph.; Jérôme, R. Brédas, J.L.; Lazzaroni R. *Langmuir* **1999**, *15*, 3915.
5. Kopp-Marsaudon, S.; Leclère, Ph.; Dubourg, F.; Lazzaroni, R.; Aimé, J.P. *Langmuir* **2000**, *16*, 8432.
6. Rasmont, A.; Leclère, Ph.; Doneux, C.; Lambin, G.; Tong, J.D.; Jérôme, R.; Brédas, J.L.; Lazzaroni, R. *Colloids and Surfaces B: Biointerfaces* **2000**, *19*, 381.
7. Konrad, M.; Knoll, A.; Krausch, G.; Magerle, R. *Macromolecules* **2000**, *33*, 5518.
8. Albrecht, T.R.; Grütter, P.; Horne, D.; Rugard D. *J. App. Phys.* **1991**, *69*, 668.
9. Zhong, Q.; Inniss, D.; Kjoller K.; Elings, V.B. *Surf. Sci.* **1993**, *290*, L688.
10. Knoll, A.; Magerle, R.; Krausch, G. *Macromolecules* **2001**, *34*, 4159.
11. Cleveland, J.P.; Anczykowski, B., Schmid, A.E.; Elings V.B. *Appl. Phys. Lett.* **1998**, *72*, 2613.
12. Garcia, R., San Paulo, A. *Phys. Rev. B* **1999**, *60*, 4961.
13. Dubourg, F., Aimé, J.P., Marsaudon, S., Boisgard, R., and Leclère, Ph. *Eur. Phys. J. E*, **2001**, *6*, 49.

14. Dubourg, F., Marsaudon, S., Leclère, Ph., Lazzaroni, R., and Aimé, J.P., *Eur. Phys. J. E*, **2001**, 6, 387.
15. Leclère, Ph., Dubourg, F., Kopp-Marsaudon, S., Brédas, J.L., Lazzaroni, R., Aimé.J.P., *Appl. Surf. Sc.*, **2002**, 188, 524.
16. Mayer, J.M. ; Kaplan D.L., *Trends in Polymer* **1994**, 2, 227.
17. Walheim, S. ; Böltau, M. ; Mlynek J. ; Krausch, G. ; Steiner, U., *Macromolecules*, **1999**, 30, 4995.
18. Chen, J.T.; Thomas, E.L.; Ober, C.K.; Mao, G.-P. *Science* **1996**, 273, 343 ; Radzilowski, L.H.; Stupp, S.I. *Macromolecules* **1994**, 27, 7747; Radzilowski, L.H.; Carragher, B.O.; Stupp, S.I. *Macromolecules* **1997**, 30, 2110. Jenekhe, S.A.; Chen, X.L. *Science* **1998**, 279, 1903.
19. Ruokolainen, J.; Mäkinen, R.; Torkkeli, M.; Mäkelä, T.; Serimaa, R.; ten Brinke, G.; Ikkala, O. *Science* **1998**, 280, 557.
20. Setayesh, S.; Marsitzky, D.; and Müllen K., *Macromolecules* **2000**, 33, 2016.
21. Henze, O. ; Parker, D. ; Feast, W.J., *J. Mater. Chem.* **2003**, 13, 1269.
22. Pantoustier, N., Lepoittevin, B., Alexandre, M., Calberg, C., Jérôme, R., Dubois, Ph., *Macromol. Symp.*, **2002**, 183, 95.
23. Lepoittevin, B., Pantoustier, N., Devalkenaere, M., Alexandre, M., Kubies, D. ; Calberg, C., Jérôme, R., and Dubois, Ph., *Macromolecules*, **2002**, 35, 8385.
24. Viville, P. ; Lazzaroni, R. ; Pollet, E. ; Alexandre, M. ; Dubois, Ph. ; Borgia, G. ; and Pireaux, J.J. *Langmuir*, **2003**, 19, 9425.